

Ring Oscillators Under Nonlinear Coupling: Bifurcation and Chaos

Hrishikesh Mondal¹, Arghya Pathak²,
Tanmoy Banerjee³, and Mrinal Kanti Mandal^{2†}, Non-members

ABSTRACT

The dynamics of two non-linearly coupled ring oscillators are examined in this study. Each ring oscillator consists of three-stage inverters, coupled through a resistor and diode. The system is mathematically modeled by non-linear differential equations. A numerical phase plane, bifurcation, and quantitative measures, like the Lyapunov exponent, confirm the transition from periodic to chaotic oscillation in a broad parameter zone. The system is implemented in a prototype hardware electronic circuit with bifurcation and chaos observed experimentally. This circuit can be used in practical applications such as cryptography and random number generation.

Keywords: Ring Oscillator, Nonlinear Coupling, Bifurcation, Chaos, Electronic Circuit

1. INTRODUCTION

Understanding the dynamics of ring oscillators is an important research topic since they play a crucial role in engineering and biology [1–4]. In electronic engineering, a ring oscillator is a multiphase system which is easy to design by cascading a number of inverters connected in a closed loop chain [5]. A ring oscillator (RO) can be designed by using single-ended or differential inverters. In the case of a single-ended inverter-based RO, the number of inverters in the closed loop chain must always be odd to support Barkhausen's oscillation criteria. However, a differential inverter-based RO can produce oscillation with an even or odd number of inverters in the closed loop chain [6, 7]. Ring oscillators have wide applications in different electronic systems, such as clock signal generation [8], FM demodulation

[9], frequency synthesizing [10–12], temperature sensing [13], etc.

The characteristics of ring oscillators [14, 15] and their applications in different fields of electronics are well documented in the literature. However, the dynamic RO model is essentially nonlinear and difficult, if not impossible, to solve exactly. For a complete understanding of the dynamics of a RO one must apply nonlinear bifurcation and chaos tools [16–18]. However, understanding the nonlinear behavior of an RO is very much limited in the literature and the appearance of bifurcation and chaos in RO has not received much attention [1, 19–21].

The motivation for studying the nonlinear behavior of ROs is two-fold. First, apart from man-made electronic circuits, ROs are also found in biological systems. For example, in a synthetic genetic repressilator, three genes in bacteria repress each other and combined behave like a ring oscillator [2]. As with most natural oscillators, genetic oscillators also work in coupled mode, therefore, some studies have explored the collective dynamics of coupled gene-based ring oscillators. In [3, 4], the dynamics of two linearly coupled synthetic genetic ROs were studied in detail. The authors reported the occurrence of multistability, quasiperiodicity, and chaos. However, the effect of nonlinear coupling in genetic ROs has not been explored. Furthermore, experimental observations of the coupled ROs collective dynamics in the biological domain are still lacking.

The second motivation comes from the application potentiality of chaos. In this context the most celebrated chaotic circuit is the Chua, establishing that apart from their academic interests, chaotic circuits can serve in the application of cryptography, random number generation, and chaotic communications [22–26]. In this connection, autonomous Boolean network-based chaos generators open the path to high frequency chaos in a flexible setup [27, 28].

Ring oscillators are also found to be potential chaos generators that can be implemented in IC form. In this endeavor, Hosokawa and Nishio [19] first proposed that when coupled through a combination of cross-coupled diodes, two three-stage ROs are capable of producing a chaotic signal. Since a chaotic signal is aperiodic in nature, it has no regular temporal zero crossings. Thus, it can generate large intrinsic jitter and may be treated as the potential source of entropy for generating a true random number (TRN), an idea implemented by Çiçek

Manuscript received on May 25, 2022; revised on July 1, 2022; accepted on August 24, 2022. This paper was recommended by Associate Editor Kriangkrai Sooksood.

¹The author is with the Department of Physics, Durgapur Government College, Durgapur, India.

²The authors are with the Department of Physics, National Institute of Technology, Durgapur, India.

³The author is with the Chaos and Complex Systems Research Laboratory, Department of Physics, University of Burdwan, Burdwan, India.

[†]Corresponding author: mrinalkanti.mandal@phy.nitdgp.ac.in

©2023 Author(s). This work is licensed under a Creative Commons Attribution-NonCommercial-NoDerivs 4.0 License. To view a copy of this license visit: <https://creativecommons.org/licenses/by-nc-nd/4.0/>.

Digital Object Identifier: 10.37936/ecti-ec.2023211.248668

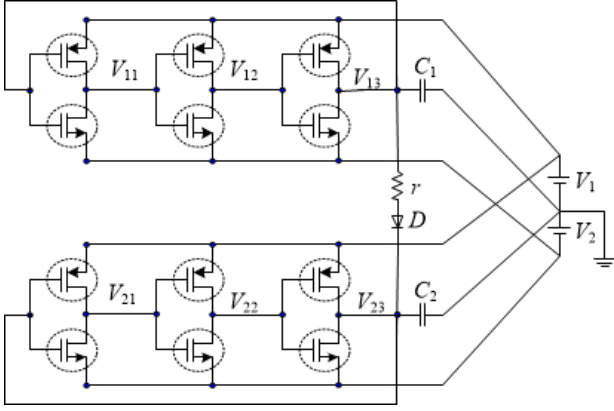


Fig. 1: Circuit diagram of two nonlinearly coupled ring oscillators. Each RO consists of three MOS inverters. D is a pn junction diode, V_1 and V_2 are bias voltages.

and Dündar [29]. Minati [20] confirmed the generation of controllable chaos by making the current starving of the 3, 5, and 7 stage ROs which were coupled through diodes of diverse coupling strengths, enabled through pass-gates.

Motivated by the foregoing, the behavior of two nonlinearly coupled ROs are studied in this paper, considering three-stage ROs with single-ended inverters. The nonlinearly coupled ROs are modeled by nonlinear differential equations. The dynamics of the system are explored both numerically and experimentally. This study shows the chaotic behaviors of coupled RO circuits in a broad range of parameter values. The transition route from non-chaotic to chaotic circuit behavior is also studied through a bifurcation diagram and Lyapunov exponent spectrum. The experimental results reveal good qualitative agreement with the numerical results.

The organization of this paper is as follows: Section 2 describes the mathematical model of the system. Section 3 presents the numerical results of the mathematical model, while the experimental results are discussed in Section 4. Finally, the main contribution of the paper is presented in Section 5.

2. MATHEMATICAL MODELING OF COUPLED RING OSCILLATORS

The schematic circuit of two nonlinearly coupled ring oscillators is shown in Fig. 1. Each RO consists of three metal oxide semiconductor (MOS)-based inverter stages. Two such ROs are coupled via a series combination of a resistor and pn junction diode. To model the circuit, the linear model of a simple inverter gate is first considered, as proposed in [19]. A single inverter of an RO can be treated as the parallel combination of a current source $G_m V_{in}$, a resistor R , and a capacitor C as shown in Fig. 2, where G_m is the gain of each inverter, R is the effective resistance in $k\Omega$ of all the gate and C in pF is the equivalent capacitance due to the parasitic effects of the individual inverter gate.

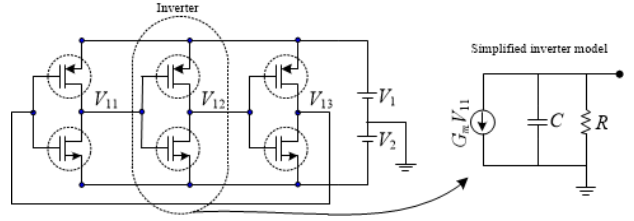


Fig. 2: Equivalent circuit diagram of an inverter gate.

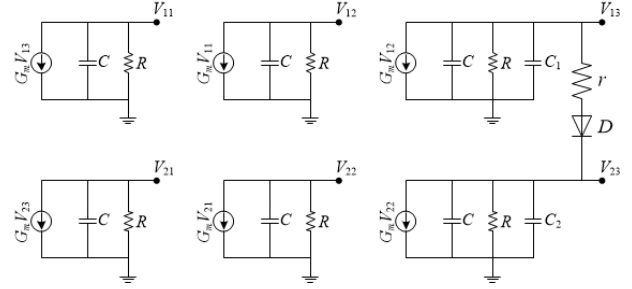


Fig. 3: Equivalent circuit of the complete circuit in Fig. 1.

The equivalent circuit of Fig. 1 according to this model is shown in Fig. 3. Applying Kirchhoff's current law (KCL) to this circuit, six voltage-current equations are developed for all nodes of the ROs. If V_{1i} s and V_{2i} s are the voltages at the nodes of the first and second RO (approximately 5 V), respectively, where i varies from 1 to 3, then they are related to each other as follows

$$\frac{dV_{11}}{dt} = -\frac{1}{RC}V_{11} - \frac{G_m}{C}V_{13} \quad (1)$$

$$\frac{dV_{12}}{dt} = -\frac{1}{RC}V_{12} - \frac{G_m}{C}V_{11} \quad (2)$$

$$\frac{dV_{13}}{dt} = -\frac{1}{RC'}V_{13} - \frac{G_m}{C'}V_{12} - \frac{i_d}{C'} \quad (3)$$

$$\frac{dV_{21}}{dt} = -\frac{1}{RC}V_{21} - \frac{G_m}{C}V_{23} \quad (4)$$

$$\frac{dV_{22}}{dt} = -\frac{1}{RC}V_{22} - \frac{G_m}{C}V_{21} \quad (5)$$

$$\frac{dV_{23}}{dt} = -\frac{1}{RC''}V_{23} - \frac{G_m}{C''}V_{22} + \frac{i_d}{C''} \quad (6)$$

$$i_d = \begin{cases} \frac{V_{13} - V_{23} - V_{th}}{r + r_d} & \text{for } (V_{13} - V_{23}) > V_{th} \\ 0 & \text{for } (V_{13} - V_{23}) \leq V_{th} \end{cases} \quad (7)$$

where $C' = C + C_1$ and $C'' = C + C_2$ are the equivalent capacitance at the coupling stage of each RO. To make the above equations dimensionless, the following can be assumed: $X_{mn} = V_{mn} / V_{th}$, $Y = ((r + r_d) / V_{th}) i_d$, $\tau = t / CR$, $\alpha = G_m R$, $\beta = C / C'$, $\gamma = C / C''$, and $\delta = R / (r + r_d)$, where X s, Y , τ , α , β , γ , and δ are all dimensionless. Accordingly, the following dimensionless

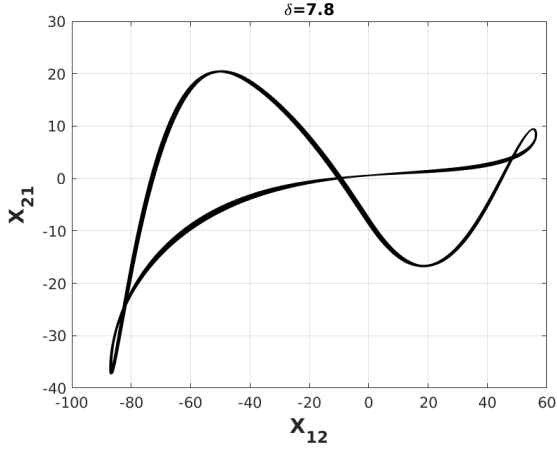


Fig. 4: Phase plane plot ($X_{12} - X_{21}$): limit cycle oscillation at $\delta = 7.8$ for $\alpha = 3.6$, $\beta = 0.1$ and $\gamma = 4$.

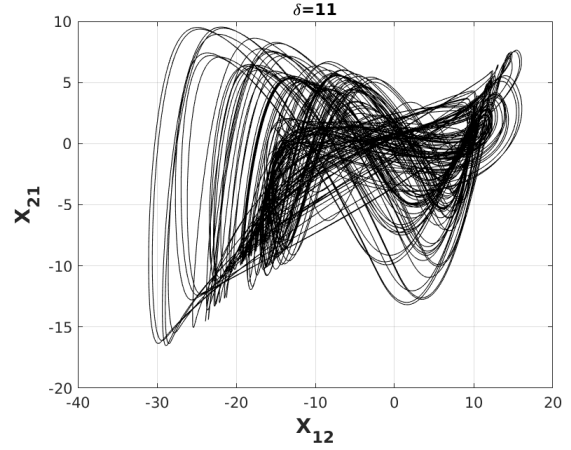


Fig. 6: Phase plane plot ($X_{12} - X_{21}$): chaotic oscillation at $\delta = 11.0$ for $\alpha = 3.6$, $\beta = 0.1$ and $\gamma = 4.0$.

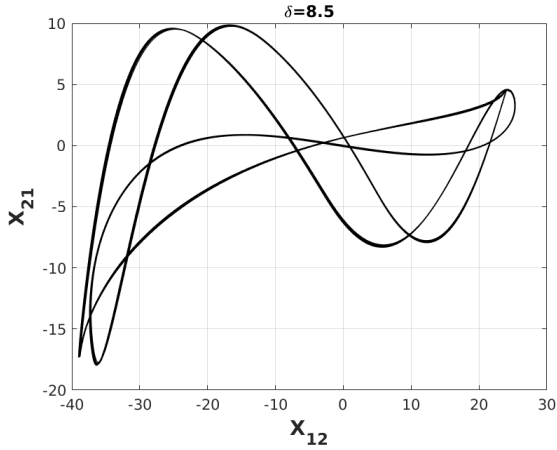


Fig. 5: Phase plane plot ($X_{12} - X_{21}$): period-2 oscillation at $\delta = 8.5$ for $\alpha = 3.6$, $\beta = 0.1$ and $\gamma = 4.0$.

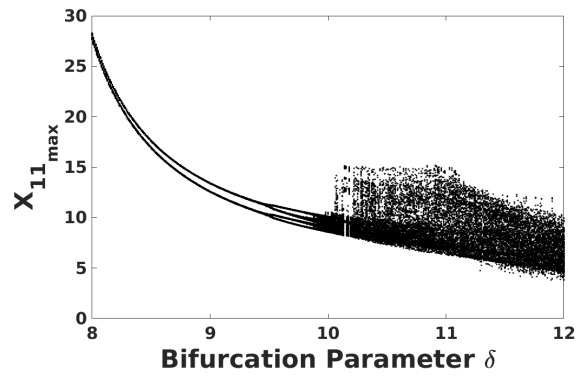


Fig. 7: Bifurcation diagram with varying δ for $\alpha = 3.6$, $\beta = 0.1$ and $\gamma = 4.0$.

equations can be obtained:.

$$\dot{X}_{11} = -X_{11} - \alpha X_{13} \quad (8)$$

$$\dot{X}_{12} = -X_{12} - \alpha X_{11} \quad (9)$$

$$\dot{X}_{13} = -\beta X_{13} - \alpha \beta X_{12} - \beta \delta Y \quad (10)$$

$$\dot{X}_{21} = -X_{21} - \alpha X_{23} \quad (11)$$

$$\dot{X}_{22} = -X_{22} - \alpha X_{21} \quad (12)$$

$$\dot{X}_{23} = -\gamma X_{23} - \alpha \gamma X_{22} + \gamma \delta Y \quad (13)$$

$$Y = \begin{cases} X_{13} - X_{23} - 1 & \text{for } (X_{13} - X_{23}) > 1 \\ 0 & \text{for } (X_{13} - X_{23}) \leq 1 \end{cases} \quad (14)$$

It is worth mentioning that Eqs. (8)–(14) represent a system which is essentially nonlinear, having piece-wise linear nonlinearity. In the next section, the dynamical

behavior of the system is explored, based on these equations.

3. NUMERICAL RESULTS

To explore the dynamics of the system, the system Eqs. (8)–(14) are solved numerically. In the numerical simulations, the fourth-order Runge-Kutta algorithm with a step size of 0.001 is used. In the bifurcation and phase space diagrams, a large number of iterations (around 10^5) are discarded to avoid transient dynamics [30, 31].

δ is varied for the following parameters $\alpha = 3.6$, $\beta = 0.1$ and $\gamma = 4.0$. It can be observed that Hopf bifurcation appears around $\delta = \delta_H = 6.8$ with a stable limit cycle. A further increase in δ makes the limit cycle distorted. Fig. 4 demonstrates the same in the $X_{12} - X_{21}$ plane for an exemplary value $\delta = 7.8$. A further increase in δ gives rise to period-doubling scenarios. A period-2 oscillation is shown in Fig. 5 at $\delta = 8.5$. Finally, chaotic oscillations appear through the period-doubling route. Fig. 6 depicts the chaotic behavior in the $X_{12} - X_{21}$ phase plane at $\delta = 11.1$.

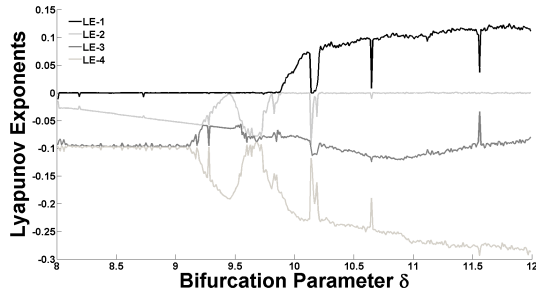


Fig. 8: Lyapunov exponent with varying δ for $\alpha = 3.6$ and $\beta = 0.1$.

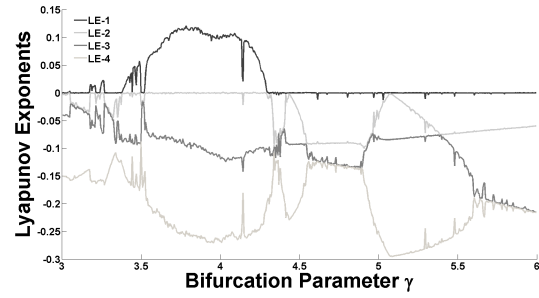


Fig. 10: Lyapunov exponent with varying γ for $\alpha = 3.6$ and $\beta = 0.1$.

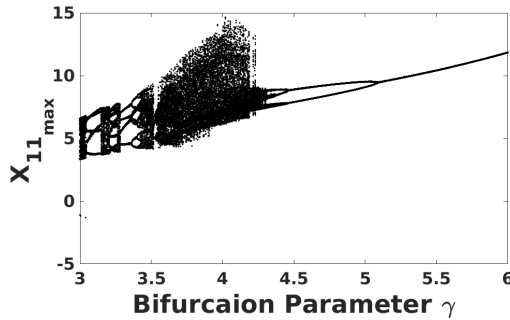


Fig. 9: Bifurcation diagram with varying γ for $\alpha = 3.6$, $\beta = 0.1$ and $\delta = 11.0$.

To explore the full spectrum of the dynamics, a bifurcation diagram is drawn with δ . Fig. 7 shows the bifurcation scenarios with δ fixed at $\alpha = 3.6$, $\beta = 0.1$ and $\gamma = 4.0$. It clearly shows a period doubling route to chaos. The chaotic behavior exists in a broad parameter region. Periodic windows are observed at $\delta \approx 10.2$ and $\delta \approx 10.7$. Also, at $\delta \approx 10.1$ a chaotic explosion is observed, giving large amplitude chaotic attractors. The corresponding Lyapunov exponent (LE) spectrum is further computed to establish the occurrence of chaos, characterized by a positive LE. See Fig. 8 for better visibility. Out of the six LEs, only four largest LEs are plotted. Periodic windows are manifested by a sudden dip in the LE spectrum to zero value.

It can be further verified that apart from δ , the variation in other parameters also gives rise to chaos. Fig. 9 shows the bifurcation diagram with γ (for $\alpha = 3.6$, $\beta = 0.1$ and $\delta = 11.0$), from which it can be observed that a decreasing γ gives rise to a period-doubling route to chaos. Here, the lower values of γ show chaos along with wider periodic windows. In the region, $3.7 \leq \gamma \leq 4.2$, chaotic attractors attain larger values.

Fig. 10 shows the corresponding LEs, supporting the bifurcation diagram in Fig. 9 and the occurrence of chaos in the system. The observation of chaotic oscillation in such a simple set up is important since it may open up the application potentiality of the circuit in random number generation, enabling the intrinsic jitter to act as the source of larger entropy [21, 32, 33].

4. EXPERIMENTAL RESULTS

The coupled circuit of Fig. 1 is designed in a hardware level set up. The individual ROs are designed using three ALD1115PAL IC chips [34], containing one p-channel and one n-channel MOSFET. The bias voltages V_1 and V_2 were chosen to be 4.90 V and -5.67 V, respectively. The substrates were also kept at the same bias voltage as the sources of each MOSFET. The frequency of each oscillator in the uncoupled condition is 2.95 MHz (measured with a spectrum analyzer, Rigol, DSA1030A 9 kHz–3 GHz). The frequency spectrum at different nodes of both oscillators were found to be identical. Two oscillators were then coupled through the series combination of a variable resistance r (10 k Ω potentiometer) and a 1N4007 diode with two capacitors, $C_1 = 150$ pF and $C_2 = 10$ pF, as depicted in Fig. 1. All the components have a 5% tolerance.

By varying the value of the resistance r , the transition of the oscillator output from the non-chaotic to chaotic mode was observed through a period-doubling cascade (note that the parameter δ depends upon r , cf. $\delta = R / (r + r_d)$). The details of the experimental phase plane plots in the $V_{12} - V_{21}$ plane are shown in Figs. 11 to 13 with varying r .

Fig. 11 shows the period-1 oscillation at $r = 8.5$ k Ω . A further decrease in r (equivalent to an increase in δ) results in period-doubling bifurcation. Fig. 12 shows a period-2 oscillation at $r = 6.3$ k Ω . A chaotic oscillation appears at a much lower value of r . Fig. 13 shows the experimental chaotic attractor at $r = 1.2$ k Ω . It should be noted that the experimental phase plane plots in Figs. 11 to 13 are in qualitative agreement with the numerical results in Figs. 4 to 6.

Apart from the experimental phase plane plots, to support bifurcation and chaos, the corresponding power-frequency spectrum is measured with a spectrum analyzer. Fig. 14 shows the frequency spectrum of period-1 oscillation of V_{12} at $r = 8.5$ k Ω . It shows a central frequency at 2.5 MHz. Period-2 oscillation at $r = 6.3$ k Ω is characterized by the appearance of two additional peaks in the frequency spectrum (see Fig. 15).

Finally, the broad and continuous frequency spectrum confirms the occurrence of chaos in the circuit. Fig. 16

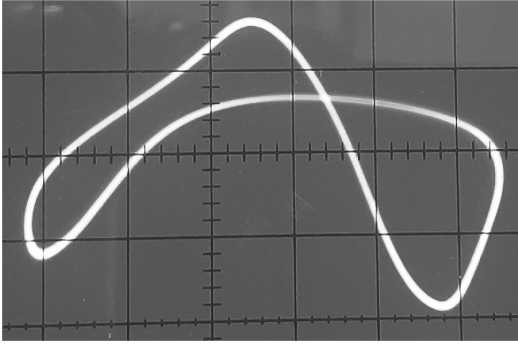


Fig. 11: Experimental phase portrait of $V_{12} - V_{21}$: Period-1 for $r = 8.5 \text{ k}\Omega$.

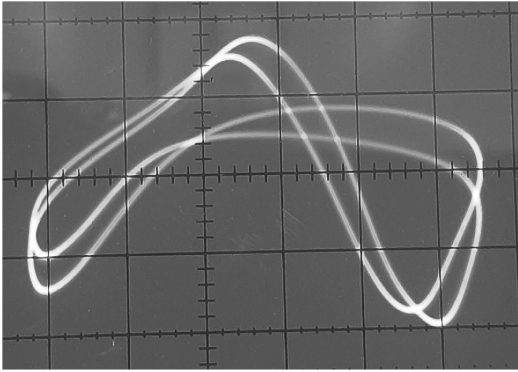


Fig. 12: Experimental phase portrait of $V_{12} - V_{21}$: Period-2 for $r = 6.3 \text{ k}\Omega$.

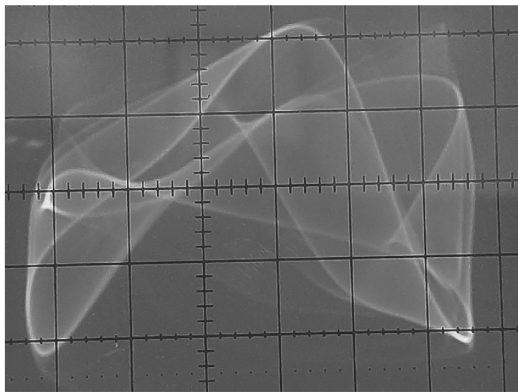


Fig. 13: Experimental phase portrait of $V_{12} - V_{21}$: Chaos for $r = 1.2 \text{ k}\Omega$.

exhibits the frequency spectrum of the chaotic signal at $r = 1.2 \text{ k}\Omega$. It can be observed that about 90% of the power is concentrated around 2.5 MHz frequency, which is the center frequency of the sinusoidal oscillation of the circuit. Moreover, in a real hardware setup, parameter

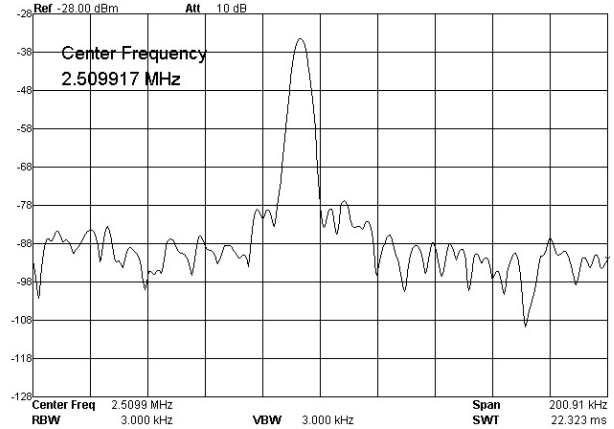


Fig. 14: Frequency spectrum of V_{12} : Period-1 for $r = 8.5 \text{ k}\Omega$.

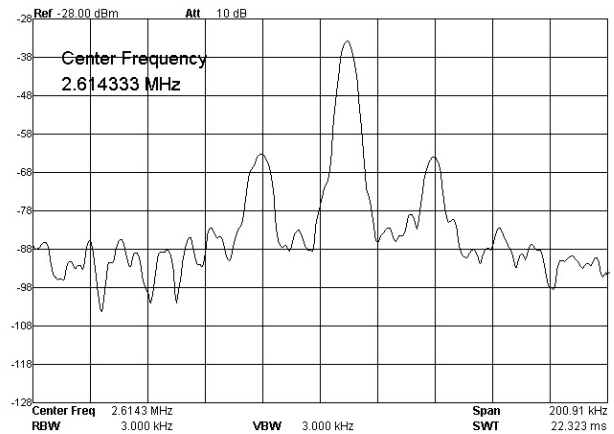


Fig. 15: Frequency spectrum of V_{12} : Period-2 for $r = 6.3 \text{ k}\Omega$.

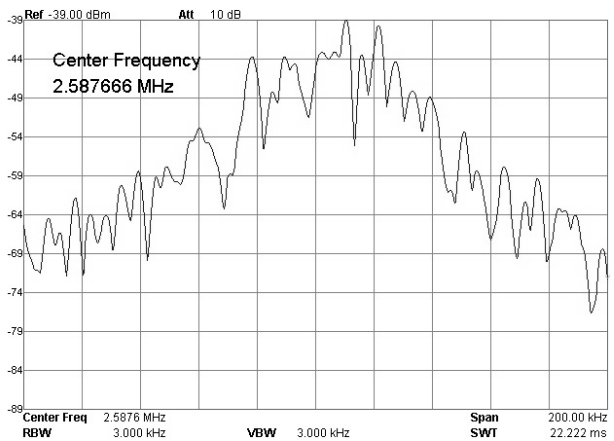


Fig. 16: Frequency spectrum of V_{12} : Chaos for $r = 1.2 \text{ k}\Omega$.

mismatch and fluctuations are inevitable.

Despite this, the experimental results in this study are qualitatively equivalent to the numerical results from the mathematical model. This shows the robustness of our hardware circuit. We checked the period doubling path to chaos for several sets of circuit parameters and obtained a qualitatively equivalent result.

5. CONCLUSION

This paper explores the nonlinear dynamics of two nonlinearly coupled ROs and the system modeled using equivalent circuit-based analysis. The numerical results and quantitative measures established that the circuit exhibited bifurcation and chaos in a broad parameter zone. The circuit was implemented in a hardware experiment and experimentally the chaotic dynamics observed. In the experiment, chaotic behavior was also established through a broad and continuous frequency spectrum.

Apart from exploring the detailed nonlinear dynamics, this study provides a simple circuit using off-the-shelf electronic components for demonstrating bifurcation and chaos in an RO. This circuit can serve as a prototype for verifying the analytical results of biological ROs [2–4]. The experimental setup can be extended to understand the noisy dynamics of ROs potentially revealing several unexplored dynamics of biological and physical ROs.

In the context of RO-based chaotic circuits, previous studies have either used numerical simulations [19] or a complex experimental setup [20] to observe chaotic behaviors. This study reveals that simple nonlinearly coupled ROs can be used to generate strong chaos in the application of random number generation and cryptography [35]. Ring oscillator-based chaos generators have clear advantages over existing operational amplifier-based chaotic oscillators [36–41] since the former is easy to design with CMOS technology [1]. This study focuses only on the chaotic dynamics of the coupled system. Therefore, the circuit for obtaining maximum frequency or least power consumption is not optimized: efforts in this direction deserve separate study.

Moreover, studies can be carried out on the cooperative dynamics of ROs, such as synchronization [42–44] and symmetry-breaking [45] phenomena. Moreover, the observation of hidden oscillations [46, 47] in ROs would be an interesting topic for future research.

REFERENCES

- [1] L. Minati *et al.*, “Current-starved cross-coupled CMOS inverter rings as versatile generators of chaotic and neural-like dynamics over multiple frequency decades,” *IEEE Access*, vol. 7, pp. 54 638–54 657, 2019.
- [2] M. B. Elowitz and S. Leibler, “A synthetic oscillatory network of transcriptional regulators,” *Nature*, vol. 403, no. 6767, pp. 335–338, Jan. 2000.
- [3] E. H. Hellen and E. Volkov, “Emergence of multistability and strongly asymmetric collective modes in two quorum sensing coupled identical ring oscillators,” *Chaos: An Interdisciplinary Journal of Nonlinear Science*, vol. 30, no. 12, Dec. 2020, Art. no. 121101.
- [4] E. H. Hellen and E. Volkov, “How to couple identical ring oscillators to get quasiperiodicity, extended chaos, multistability, and the loss of symmetry,” *Communications in Nonlinear Science and Numerical Simulation*, vol. 62, pp. 462–479, Sep. 2018.
- [5] M. K. Mandal and B. C. Sarkar, “Ring oscillators: Characteristics and applications,” *Indian Journal of Pure & Applied Physics*, vol. 48, pp. 136–145, Feb. 2010.
- [6] J. Jalil, M. B. I. Reaz, and M. A. M. Ali, “CMOS differential ring oscillators: Review of the performance of CMOS ROs in communication systems,” *IEEE Microwave Magazine*, vol. 14, no. 5, pp. 97–109, Jul. 2013.
- [7] A. Koithyar and T. K. Ramesh, “Modeling of the submicron CMOS differential ring oscillator for obtaining an equation for the output frequency,” *Circuits, Systems, and Signal Processing*, vol. 40, no. 4, pp. 1589–1606, Apr. 2021.
- [8] J. Cortadella, M. Lupon, A. Moreno, A. Roca, and S. S. Sapatnekar, “Ring oscillator clocks and margins,” in *22nd IEEE International Symposium on Asynchronous Circuits and Systems (ASYNC)*, Porto Alegre, Brazil, 2016, pp. 19–26.
- [9] M. K. Mandal and B. C. Sarkar, “Characteristics of a variable length ring oscillator and its use in PLL based systems,” *International Journal of Electronics*, vol. 93, no. 1, pp. 29–40, Jan. 2006.
- [10] A. Khashaba, A. Elkholy, K. M. Megawer, M. Ahmed, and P. K. Hanumolu, “A 5GHz 245firms 8mW ring oscillator-based digital frequency synthesizer,” in *2019 IEEE Custom Integrated Circuits Conference (CICC)*, Austin, TX, USA, 2019.
- [11] B. C. Sarkar and M. K. Mandal, “A ring oscillator based frequency synthesizer without using frequency divider,” *International Journal of Electronics*, vol. 94, no. 2, pp. 123–136, Feb. 2007.
- [12] T. Banerjee and B. C. Sarkar, “Chaos, intermittency and control of bifurcation in a ZC_2 -DPLL,” *International Journal of Electronics*, vol. 96, no. 7, pp. 717–732, Jul. 2009.
- [13] S.-S. Woo, J.-H. Lee, and S. Cho, “A ring oscillator-based temperature sensor for u-healthcare in $0.13\mu\text{m}$ cmos,” in *2009 International SoC Design Conference (ISOCC)*, Busan, Korea, 2009, pp. 548–551.
- [14] A. Hajimiri, S. Limotyrakis, and T. Lee, “Jitter and phase noise in ring oscillators,” *IEEE Journal of Solid-State Circuits*, vol. 34, no. 6, pp. 790–804, Jun. 1999.
- [15] A. Hajimiri and T. H. Lee, *The Design of Low Noise Oscillators*. Boston, MA, USA: Springer, 1999.
- [16] H. G. Schuster and W. Just, *Deterministic Chaos: An Introduction*, 4th ed. Weinheim, Germany: Wiley-VCH Verlag, 2005.
- [17] D. Biswas and T. Banerjee, *Time-Delayed Chaotic Dynamical Systems: From Theory to Electronic Experiment*. Cham, Switzerland: Springer, 2017.
- [18] T. Banerjee, B. Karmakar, and B. C. Sarkar, “Single amplifier biquad based autonomous electronic oscillators for chaos generation,” *Nonlinear Dynamics*, vol. 62, no. 4, pp. 859–866, Dec. 2010.

- [19] Y. Hosokawa and Y. Nishio, "Simple chaotic circuit using CMOS ring oscillators," *International Journal of Bifurcation and Chaos*, vol. 14, no. 07, pp. 2513–2524, Jul. 2004.
- [20] L. Minati, "Experimental implementation of networked chaotic oscillators based on cross-coupled inverter rings in a CMOS integrated circuit," *Journal of Circuits, Systems and Computers*, vol. 24, no. 09, 2015, Art. no. 1550144.
- [21] E. Farcot, S. Best, R. Edwards, I. Belgacem, X. Xu, and P. Gill, "Chaos in a ring circuit," *Chaos: An Interdisciplinary Journal of Nonlinear Science*, vol. 29, no. 4, Apr. 2019, Art. no. 043103.
- [22] T. Matsumoto, L. Chua, and M. Komuro, "The double scroll," *IEEE Transactions on Circuits and Systems*, vol. 32, no. 8, pp. 797–818, Aug. 1985.
- [23] M. Kennedy, "Three steps to chaos. II. a Chua's circuit primer," *IEEE Transactions on Circuits and Systems I: Fundamental Theory and Applications*, vol. 40, no. 10, pp. 657–674, Oct. 1993.
- [24] N. Wang, C. Li, H. Bao, M. Chen, and B. Bao, "Generating multi-scroll Chua's attractors via simplified piecewise-linear Chua's diode," *IEEE Transactions on Circuits and Systems I: Regular Papers*, vol. 66, no. 12, pp. 4767–4779, Dec. 2019.
- [25] N. Wang, G. Zhang, N. Kuznetsov, and H. Bao, "Hidden attractors and multistability in a modified Chua's circuit," *Communications in Nonlinear Science and Numerical Simulation*, vol. 92, Jan. 2021, Art. no. 105494.
- [26] T. Banerjee, "Single amplifier biquad based inductor-free Chua's circuit," *Nonlinear Dynamics*, vol. 68, no. 4, pp. 565–573, Jun. 2012.
- [27] J. M. Munoz-Pacheco, T. García-Chávez, V. R. Gonzalez-Diaz, G. de La Fuente-Cortes, and L. del Carmen del Carmen Gómez-Pavón, "Two new asymmetric boolean chaos oscillators with no dependence on incommensurate time-delays and their circuit implementation," *Symmetry*, vol. 12, no. 4, 2020, Art. no. 506.
- [28] M. Park, J. C. Rodgers, and D. P. Lathrop, "True random number generation using CMOS boolean chaotic oscillator," *Microelectronics Journal*, vol. 46, no. 12, pp. 1364–1370, Dec. 2015.
- [29] İhsan Çiçek and G. Dündar, "A hardware efficient chaotic ring oscillator based true random number generator," in *2011 18th IEEE International Conference on Electronics, Circuits, and Systems*, Beirut, Lebanon, 2011, pp. 430–433.
- [30] N. Wang, G. Zhang, N. Kuznetsov, and H. Li, "Generating grid chaotic sea from system without equilibrium point," *Communications in Nonlinear Science and Numerical Simulation*, vol. 107, Apr. 2022, Art. no. 106194.
- [31] N. Wang, G. Zhang, and H. Bao, "Bursting oscillations and coexisting attractors in a simple memristor-capacitor-based chaotic circuit," *Nonlinear Dynamics*, vol. 97, no. 2, pp. 1477–1494, Jul. 2019.
- [32] P. Grassberger and I. Procaccia, "Measuring the strangeness of strange attractors," *Physica D: Nonlinear Phenomena*, vol. 9, no. 1–2, pp. 189–208, Oct. 1983.
- [33] S. N. Dhanuskodi, A. Vijayakumar, and S. Kundu, "A chaotic ring oscillator based random number generator," in *2014 IEEE International Symposium on Hardware-Oriented Security and Trust (HOST)*, Arlington, VA, USA, 2014, pp. 160–165.
- [34] "ALD1115," Advanced Linear Devices, Inc., Sunnyvale, California, USA, 2021. [Online]. Available: <http://www.aldinc.com/pdf/ALD1115.pdf>
- [35] C. Volos, I. Kyprianidis, and I. Stouboulos, "Image encryption process based on chaotic synchronization phenomena," *Signal Processing*, vol. 93, no. 5, pp. 1328–1340, May 2013.
- [36] I. Kyprianidis, I. Stouboulos, and C. Volos, *New Research Trends in Nonlinear Circuits: Design, Chaotic Phenomena and Applications*. New York, USA: Nova Science Publishers, 2014.
- [37] T. Banerjee, B. Karmakar, and B. C. Sarkar, "Chaotic electronic oscillator from single amplifier biquad," *AEÜ - International Journal of Electronics and Communications*, vol. 66, no. 7, pp. 593–597, Jul. 2012.
- [38] C. Volos, J.-O. Maaïta, S. Vaidyanathan, V.-T. Pham, I. Stouboulos, and I. Kyprianidis, "A novel four-dimensional hyperchaotic four-wing system with a saddle-focus equilibrium," *IEEE Transactions on Circuits and Systems II: Express Briefs*, vol. 64, no. 3, pp. 339–343, Mar. 2017.
- [39] V.-T. Pham, A. Ouannas, C. Volos, and T. Kapitaniak, "A simple fractional-order chaotic system without equilibrium and its synchronization," *AEÜ - International Journal of Electronics and Communications*, vol. 86, pp. 69–76, Mar. 2018.
- [40] S. Sabarathinam, C. K. Volos, and K. Thamilmaran, "Implementation and study of the nonlinear dynamics of a memristor-based Duffing oscillator," *Nonlinear Dynamics*, vol. 87, no. 1, pp. 37–49, Jan. 2017.
- [41] V. Varshney, S. Sabarathinam, A. Prasad, and K. Thamilmaran, "Infinite number of hidden attractors in memristor-based autonomous Duffing oscillator," *International Journal of Bifurcation and Chaos*, vol. 28, no. 01, Jan. 2018, Art. no. 1850013.
- [42] T. Banerjee and D. Biswas, "Synchronization in hyperchaotic time-delayed electronic oscillators coupled indirectly via a common environment," *Nonlinear Dynamics*, vol. 73, no. 3, pp. 2025–2048, Aug. 2013.
- [43] E. Schöll, "Synchronization patterns and chimera states in complex networks: Interplay of topology and dynamics," *The European Physical Journal Special Topics*, vol. 225, no. 6–7, pp. 891–919, Sep. 2016.
- [44] T. Banerjee, D. Biswas, D. Ghosh, E. Schöll, and A. Zakharova, "Networks of coupled oscillators: From phase to amplitude chimeras," *Chaos: An Interdisciplinary Journal of Nonlinear Science*, vol. 28,

no. 11, Nov. 2018, Art. no. 113124.

- [45] T. Banerjee, D. Biswas, D. Ghosh, B. Bandyopadhyay, and J. Kurths, "Transition from homogeneous to inhomogeneous limit cycles: Effect of local filtering in coupled oscillators," *Physical Review E*, vol. 97, no. 4, Apr. 2018, Art. no. 042218.
- [46] G. A. Leonov and N. V. Kuznetsov, "Hidden attractors in dynamical systems. from hidden oscillations in Hilbert–Kolmogorov, Aizerman, and Kalman problems to hidden chaotic attractor in Chua circuits," *International Journal of Bifurcation and Chaos*, vol. 23, no. 01, Jan. 2013, Art. no. 1330002.
- [47] G. Leonov, N. Kuznetsov, and V. Vagitsev, "Localization of hidden Chua's attractors," *Physics Letters A*, vol. 375, no. 23, pp. 2230–2233, Jun. 2011.



Hrishikesh Mondal received the B.Sc. degrees in Physics (Hons.) and M.Sc. in Physics from the University of Burdwan, Burdwan, West Bengal, India in 1998 and 2000 respectively. Presently, he is an Assistant Professor of Physics in Durgapur Government College and pursuing Ph.D. from National Institute of Technology, Durgapur, West Bengal, India. He has published three research papers in national and international journals.



Arghya Pathak received his B.Sc. degree in Physics from J.K College Purulia (The University of Burdwan), India in 2012 and M.Sc. in Physics from National Institute of Technology Durgapur, India in 2014. Presently, he is pursuing his Doctoral research work. His research interests include image processing, sparse representation of signals, data security and cryptography. He has published one paper in international journals.



Tanmoy Banerjee received the B.Sc. degree in Physics (Hons.) from the University of Burdwan, Burdwan, West Bengal, India in 1998, and the M.Sc. and Ph.D. degrees from the same University in 2000 and 2008, respectively. Presently, he is a Professor in the Department of Physics, the University of Burdwan, Burdwan, West Bengal, India. He has published more than 80 international journal papers and 50 conference papers in proceeding. His research interests include nonlinear science, symmetry-breaking in coupled oscillators, oscillation suppression: amplitude death and oscillation death, nonlinear dynamics in the quantum regime, chaotic dynamical systems, nonlinear electronic circuits and systems, and mathematical biology. He is a fellow of IETE (Institute of Electronics and Telecommunication Engineers).



Mrinal Kanti Mandal received the B.Sc. degree in Physics (Hons.) from Burdwan University, India in 1998, and the M.Sc. and Ph.D. degrees from the same University in 2000 and 2008 respectively. Presently, he is an Associate Professor in the Department of Physics, National Institute of Technology, Durgapur, India. He has published more than 45 international journal papers and 35 conference papers in proceeding. His research interests include design of electronic circuits and systems, nonlinear dynamics and chaos, cryptography and image processing. He is a reviewer of *Nonlinear Dynamics*, *Security and Communication Networks*, *International Journal of Electronics*, *Indian Journal of Pure and Applied Physics*, *Indian Journal of Physics*, etc. He is a fellow of IETE (Institute of Electronics and Telecommunication Engineers). He is a member of IEEE, and life members of IPS and IAPT. His bio-data has been included in the database of science and technology chapter of "Marquis Who's Who" since 2010 edition.